

Influence of Nano-Finishing Process on Fatigue Life of Stainless Steel-304

S. Dineshkumar¹, P. Palanikumar², R. Praveen³, T. Thilak⁴, P. Kasinatha Pandian⁵

¹ Department of Mechanical Engineering, KarpagaVinayaga College of Engineering and Technology, India - 603 308

² Department of Automobile Engineering, KarpagaVinayaga College of Engineering and Technology, India - 603 308

³Department of Robotic and Automation, KarpagaVinayaga College of Engineering and Technology, India Pin: 603 308

⁴ Department of Physics, KarpagaVinayaga College of Engineering and Technology, India Pin: 603 308

⁵ Department of Civil Engineering, KarpagaVinayaga College of Engineering and Technology, India Pin: 603 308

Corresponding author email: pvnandha@gmail.com,

Abstract— Being labor-intensive and challenging to regulate, precision finishing of internal surfaces and complicated geometries is always an issue. In order to achieve the desired geometrical accuracy and surface qualities, undesired excess material is often removed from the work piece surface using small multiple cutting edges of abrasives. The existing traditional finishing procedures alone are unable to produce the necessary surface finish and other characteristics due to the introduction of new challenges to machine materials (carbide, composite materials, etc.) and complex geometrical shapes of engineering components. A new method for precision finishing namely Magneto Rheological Abrasive Flow Finishing (MRAFF) was developed for fine finishing of complex interior geometries ranging from optical glasses to hard crystals using smart Magneto Rheological polishing fluid. In the viscoplastic foundation of silicone oil, ferrous powdered and cerium oxide abrasives are dispersed to create magneto rheological (MR) polishing fluid. It modifies its rheological behaviour when an external magnetic field is present. The final surface finish is achieved to the MR-polishing fluid's clever behaviour, which is used to precisely manage the finishing force. As a part of the research work, ferrous and abrasive nano particles have been prepared and analysed by scanning electron microscope (SEM) and MR-fluid also prepared by magnetic stirrer method.

Keywords: Surface roughness, Nano finishing, MRAFF, Polishing fluid.

I. INTRODUCTION

The two primary categories of micro- or nano-machining procedures are classic and cutting-edge. The majority of traditional MNM techniques use cutting tools with fixed geometry or incorporated abrasives. On the other hand, the bulk of sophisticated MNM techniques rely on loosely flowing abrasives and do not set the work piece's orientation or shape at the time of engagement. Certain MNM procedures, such as LBM, EBM, IBM, and PBM, do not fall under the abrasive-based MNM category. Only the various MNM techniques based on flowing abrasives are covered in detail in this work. Also, it suggests a universal mechanism for removing material from these processes. Over the past few decades, new, more complex finishing techniques have been created to address the shortcomings of more conventional finishing techniques, such as their higher requirement for tool hardness and their imprecise control of finishing pressures while in use. This facilitated the finishing of tougher materials and enhanced process controls over final surface properties. Finishing complex geometries by expanding the reach of abrasive to inaccessible portions of the piece surface is another restriction eased by some advance finishing

procedures using loose abrasives. In this way, newly formed finishing techniques greatly aid in meeting the demands of production in the twenty-first century.

1.1 ADVANCED SURFACE MACHINING TECHNIQUES

The Advance Surface Machining procedures may be divided into two classes to comprehend their operating principles. The first category consists of (AFF), (EMM), and Chemo Mechanical Polishing (CMP), where external control of the forces operating on the work piece during the finishing process is not possible. The second one consists of Magnetic Float Polishing, Magneto rheological Finishing, Magneto rheological Abrasive Flow Finishing, and Magnetic Abrasive Finishing (MAF, MRF, MRAFF) (MFP). By adjusting the electric current running through the magnetic coil or by adjusting the working gap when employing a permanent magnet, it is feasible to externally regulate the force applied on the work piece in these procedures. The normal force an abrasive particle normally exerts on the workpiece surface changes as a result of a change in the current flow because it alters the density of magnetic flux in the working zone. This variation in normal force affects the process's essential surface finish and finishing rate under the specified finishing conditions.

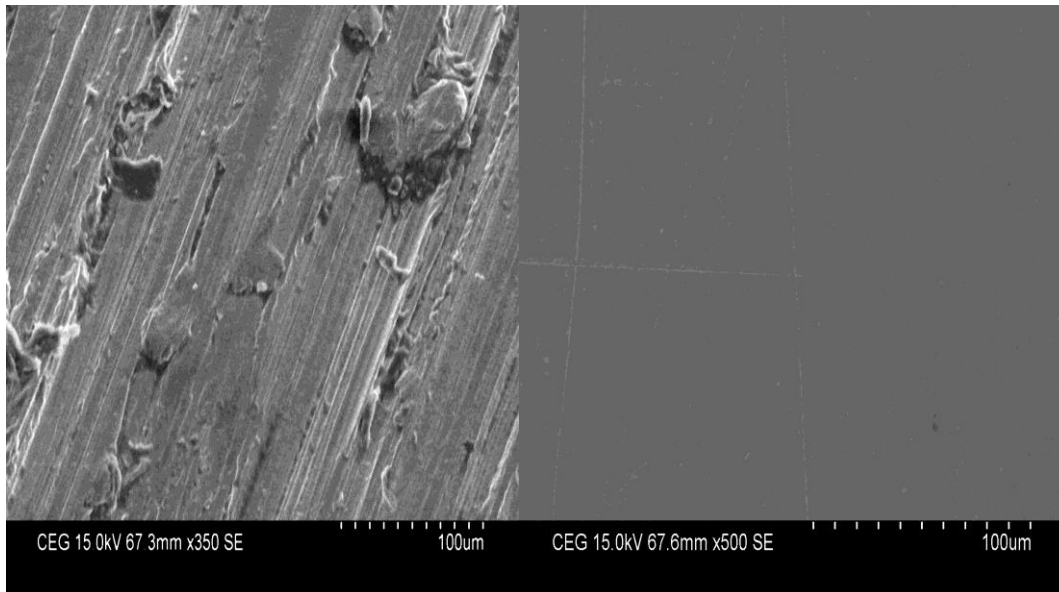
II. EXPERIMENTALWORK

2.1 EXPERIMENTAL PLANNING AND PROCEDURE

1. Preparation of Magneto rheological Fluid
2. Preparation of working specimens required for MRAFF process.
3. Experimental analysis of MRAFF process on the working Specimens by varying the process parameters.
4. Surface Roughness measurements using Tally Surface Interferometer.
5. Preparation of Fatigue test specimen (ASTM Standard) to be used in bending fatigue testing machine.
6. Analysis of influence of surface Roughness on fatigue life of 304 SS by plotting S-N curve.

2.1.1 MAGNETORHEOLOGICAL FLUID

We studied about the magneto rheological fluid to be used in our process initially. Silicon carbide particles chose as the abrasive particle and silicon oil was chose for the polymeric medium. As studied from the literature reviews the composition of the MR fluid has been determined as it contains 60% of silicon oil, 20% of silicon carbide abrasive particles, 20% of iron particles. The MR fluid was prepared for half an hour thoroughly with a mechanical stirrer till the mixture has been mixed homogenously. The work piece samples in a dimension that can be used in the process setup was made by machining in a wire cut EDM. The process parameters of this process are current, no of cycles, pressure of the MR fluid. With this we got varying combinations of the process parameters. By taguchi L9 methodology the process parameters are optimized. The nine combinations of process parameters with which we can get the best surface finish has been selected and chose for the MRAFF process. With imparting nine combinations of process parameters separately, nine work pieces have been done with the MRAFF process and the surface finish has been improved. [27-29]



(a) (b)
Figure 2.1 SEM Image of Specimen (a) before MRAFF Process (b) after MRAFF Process

The surface finishes of the work pieces were found using the Tally surf interferometer. The Scanning Electron Microscopic images of the work pieces are taken. Then our objective was to find the fatigue life of the specimen and to plot the S-N curve. Only by plotting the S-N curve we could find the fatigue life. To plot a S-N curve for a specimen with a surface finish we need at least five specimens with absolutely the same surface finish. So specimens with optimum surface finish value that is the work piece with minimum Ra value is made again with the same process parameters imparted in the machine.

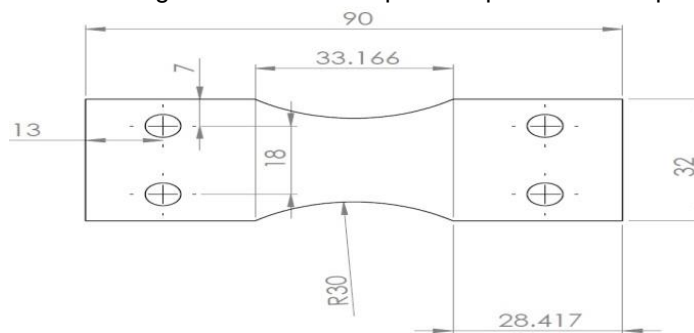


Figure 2.2 Specimen with ASTM E739

Bending fatigue machine was used to do fatigue test. Our main objective is to prove that the fatigue life of the stainless steel 304 will be improved if the surface finish of the specimen is improved. In order to demonstrate that the surface finish's fatigue life improved the specimen is improved we need to compare it with specimen having high Ra value that is less surface finish. Hence specimen with less surface finish with the same Ra value has been made. The standard specimen size (ASTM standard) to be used in the fatigue testing machine has been found out from the literature review. All the specimens to be imparted into fatigue test has been machined in the wire cut EDM according to the ASTM standard specimen size. The holes to be made in the specimen was done using the drilling machine. For all the ten specimens fatigue bend test is done. The time required for the specimen to fracture has been found out and the stress applied was also calculated using the procedure available for that bending machine. With the found out values the S-N curve has been generated for both the surface finish improved specimen

and the specimen with less surface finish. From the S-N curve generated the fatigue life of both the specimen has been found out. It has been observed that the surface finish's fatigue life improved specimen has increased to a greater level then the specimen with poor surface finish.



Figure 2.3 Fatigue Testing Specimens

Our ceo2 powder is combined with a special concoction of components to create cerium oxide slurries. Ceo2 powder is made for polishing hard-to-polish optical mirrors, lenses, and windows with extreme precision. It has also been employed for the crucial final polishing of crystal and substrates. Cerium Oxide Slurries can be used satisfactorily for synthetic lapping pitches since they are compatible with both hard and soft laps, including pads, metals, and composites.

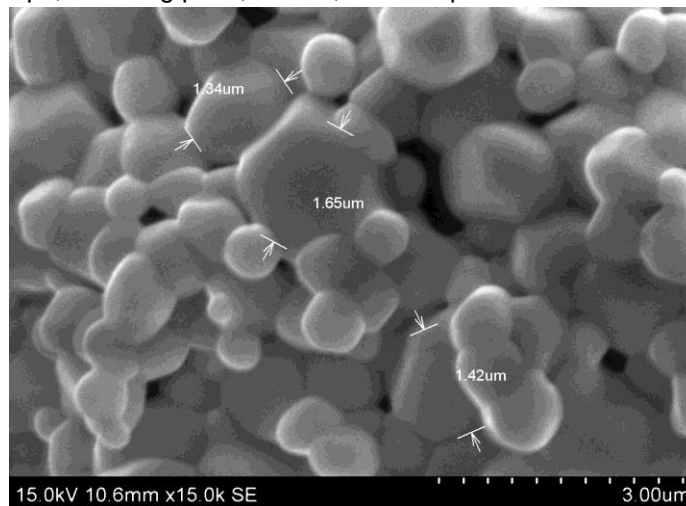


Figure 2.4SEM photograph for Micron Size Ceric oxide particles

A sample particle suspended system was chosen using carbonyl iron powder. This is due to the magnetically soft nature of carbonyl iron and its high saturation magnetization. The average tap density and particle size are 4.3 g/cm³ and 6.0 8.0 m, respectively. The amount of CI was set at twenty and forty weight percent. Other substances were applied to the fluids in order to decrease the deposition of the CI particles.

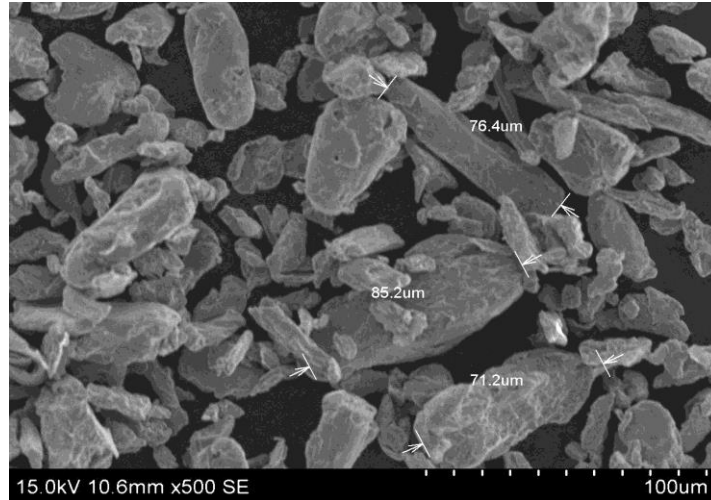


Figure 2.5SEM photograph for Micron Size ferrous particles

Carrier liquid serves as a suspension medium for the magnetized active phase particles. Moreover, the carrier liquid must mainly not react with the magnetic particles. Similar to this, the device's components and materials shouldn't react with the carrier liquid. It is crucial to take the boiling point, increased temperature vapour pressure, and freezing point into account when choosing a carrier liquid. For this reason, colourless silicone oil was used to disperse magnetorheological particles.

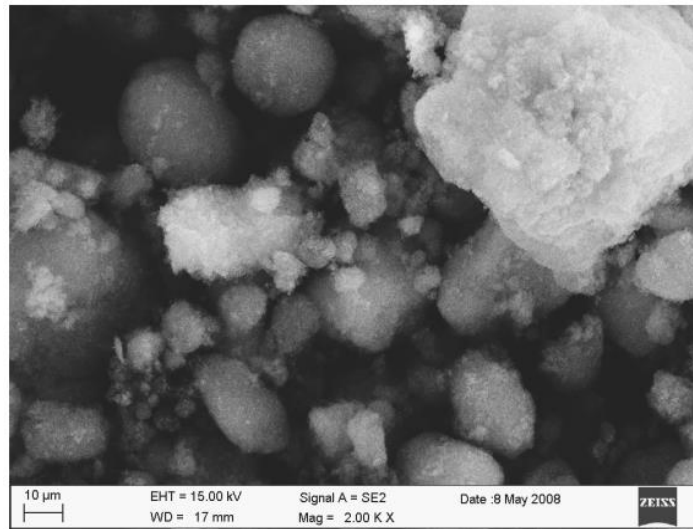


Figure 2.6SEM photograph of Silicon Oil

III. RESULTS AND DISCUSSIONS

This chapter deals with the results obtained and discussions made based on the experimental values.

The following MRAFF process parameters were studied.

1. Effect of Extrusion Pressure
2. Effect of Current
3. Effect of Number of Cycles

Table: 3.1 TAGUCHI'S L9 PARAMETERS AND ROUGHNESS VALUES

| Sl.no | Pressure (bar) | Current (A) | No.of cycles | Surface finish(Ra) nm |
|-------|----------------|-------------|--------------|-----------------------|
| 1 | 30 | 2 | 100 | 37.75 |
| 2 | 30 | 4 | 200 | 32.11 |
| 3 | 30 | 6 | 300 | 26.49 |
| 4 | 40 | 2 | 200 | 36.07 |
| 5 | 40 | 4 | 300 | 30.39 |
| 6 | 40 | 6 | 100 | 31.15 |
| 7 | 50 | 2 | 300 | 34.35 |
| 8 | 50 | 4 | 100 | 35.1 |
| 9 | 50 | 6 | 200 | 29.4 |

Here is a summary of the results based on the table:

The surface finish (Ra) generally improves with increasing number of cycles for all pressure-current combinations, except for Sl.no 6 which is an outlier.

In general, increasing the current tends to result in a better surface finish, except for Sl.no 8 which is an outlier.

Increasing the pressure does not necessarily lead to an improved surface finish, as there is no clear trend observed in the data.

It should be noted that these observations are based solely on the information provided in the table, and more detailed statistical analysis would be required to draw more definitive conclusions about the effects of these process parameters on surface finish. Additionally, it is important to consider other factors that may affect the surface finish, such as the properties of the workpiece material and the magnetic fluid used in the MRAFF process.

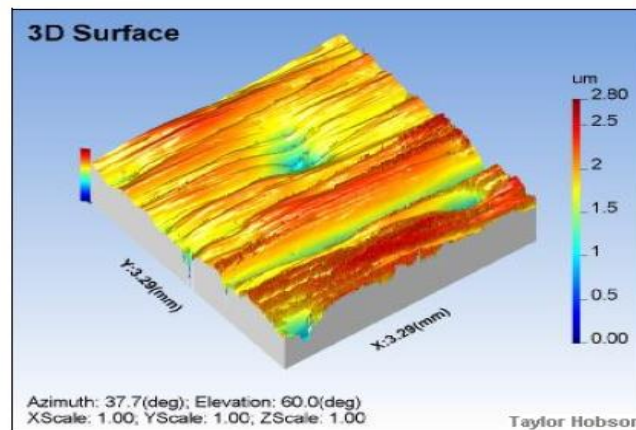


Figure 3.1 Advanced 3 D Image of Surface Finish

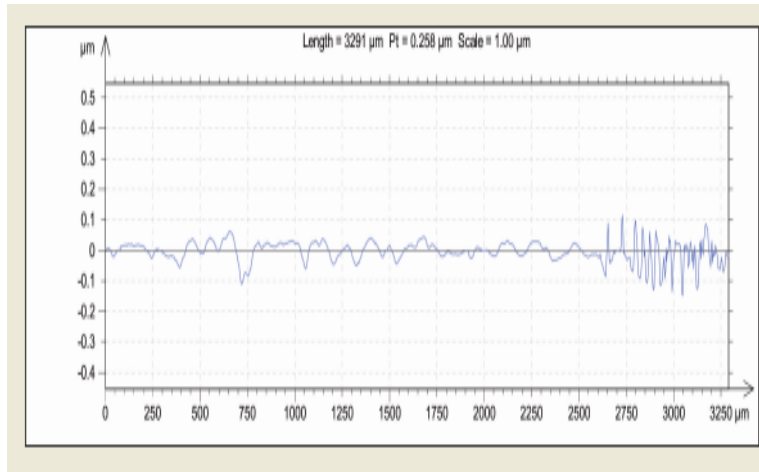


Figure 3.2 2D Graph of Surface Roughness

Table 3.2 Experiment 1 (30 bar, 2 A, 100 cycles)

| Parameter | Value (μm) |
|-----------|-------------------------|
| Ra | 0.03775 |
| Rt | 0.328425 |
| Rz | 0.2718 |
| Rz ISO | 0.2869 |
| Rmax | 0.302 |
| Rp | 0.1359 |
| RPM | 0.109475 |
| RMS | 0.041525 |

Table 3.3 Experiment 2 (30 bar, 4 A, 200 cycles)

| Parameter | Value (μm) |
|-----------|-------------------------|
| Ra | 0.03211 |
| Rt | 0.279357 |
| Rz | 0.231192 |
| Rz ISO | 0.244036 |
| Rmax | 0.25688 |
| Rp | 0.115596 |
| RPM | 0.093119 |
| RMS | 0.035321 |

Table 3.4 Experiment 3 (30 bar, 6 A, 300 cycles)

| Parameter | Value (μm) |
|-----------|-------------------------|
| Ra | 0.02649 |
| Rt | 0.230463 |
| Rz | 0.190728 |
| Rz ISO | 0.201324 |
| Rmax | 0.21192 |
| Rp | 0.095364 |
| RPM | 0.076821 |

| | |
|-----|----------|
| RMS | 0.029139 |
|-----|----------|

Table 3.5 Experiment 4 (40 bar, 2 A, 100 cycles)

| Parameter | Value (μm) |
|-----------|-------------------------|
| Ra | 0.03607 |
| Rt | 0.313809 |
| Rz | 0.259704 |
| Rz ISO | 0.274132 |
| Rmax | 0.28856 |
| Rp | 0.129852 |
| RPM | 0.104603 |
| RMS | 0.039677 |

Table 3.6 Experiment 5 (40 bar, 4 A, 300 cycles)

| Parameter | Value (μm) |
|-----------|-------------------------|
| Ra | 0.03039 |
| Rt | 0.264393 |
| Rz | 0.218808 |
| Rz ISO | 0.230964 |
| Rmax | 0.24312 |
| Rp | 0.109404 |
| RPM | 0.088131 |
| RMS | 0.033429 |

Table 3.7 Experiment 6 (40 bar, 6 A, 100 cycles)

| Parameter | Value (μm) |
|-----------|-------------------------|
| Ra | 0.03115 |
| Rt | 0.271005 |
| Rz | 0.22428 |
| Rz ISO | 0.23674 |
| Rmax | 0.2492 |
| Rp | 0.11214 |
| RPM | 0.090335 |
| RMS | 0.034265 |

Table 3.8 Experiment 7 (50 bar, 2 A, 300 cycles)

| Parameter | Value (μm) |
|-----------|-------------------------|
| Ra | 0.03435 |
| Rt | 0.298845 |
| Rz | 0.24732 |
| Rz ISO | 0.26106 |
| Rmax | 0.2748 |
| Rp | 0.12366 |
| RPM | 0.099615 |
| RMS | 0.037785 |

Table 3.9 Experiment 8 (50 bar, 4 A, 100 cycles)

| Parameter | Value (μm) |
|-----------|-------------------------|
| Ra | 0.0351 |
| Rt | 0.30537 |
| Rz | 0.25272 |
| Rz ISO | 0.26676 |
| Rmax | 0.2808 |
| Rp | 0.12636 |
| RPM | 0.10179 |
| RMS | 0.03861 |

Table 3.10 Experiment 9 (50 bar, 6 A, 200 cycles)

| Parameter | Value (μm) |
|-----------|-------------------------|
| Ra | 0.0294 |
| Rt | 0.25578 |
| Rz | 0.21168 |
| Rz ISO | 0.22344 |
| Rmax | 0.2352 |
| Rp | 0.10584 |
| RPM | 0.08526 |
| RMS | 0.03234 |

3.1. EXTRUSION PRESSURE'S IMPACT

Experiments conducted with the hydraulic pressure of 30, 40 and 50 bar with no. of cycles 100 to 300 and current 2A to 6 A for nine different cases. It was observed from the graph that there was under the experimental condition increase in surface roughness. It was observed from the graph that there was increase in surface roughness with the increase of extrusion pressure under the experimental conditions.

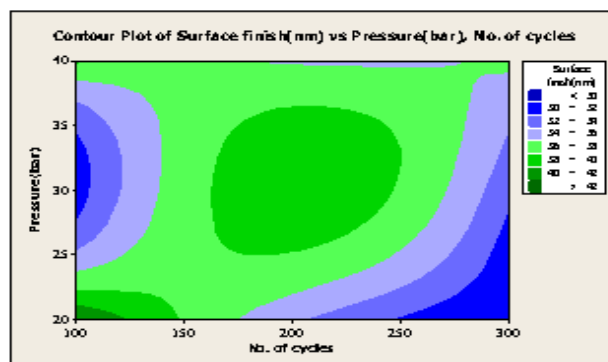


Figure 3.3 Effect of Extrusion Pressure

3.2. EFFECT OF CURRENT

From the experiment there was a finding that when the current increases from 2 to 6 Amps there was Moreover, the surface finish has made considerable progress as reduction in surface reduction Ra.

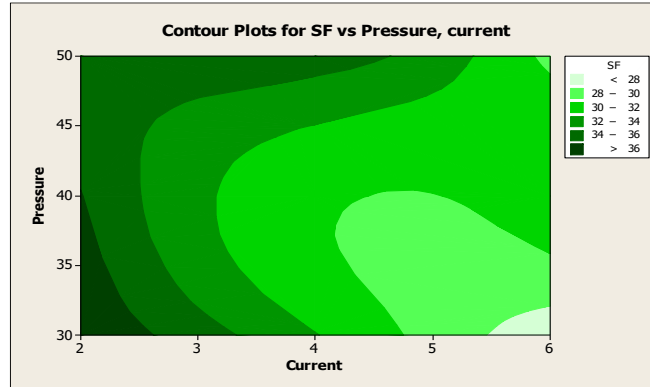


Figure 3.4 Effect of Current on Surface Finish

3.3. EFFECT OF NUMBER OF CYCLES

The work piece's surface quality is significantly impacted by the number of cycles, and the decrease in roughness value increases as the number of cycles rises.

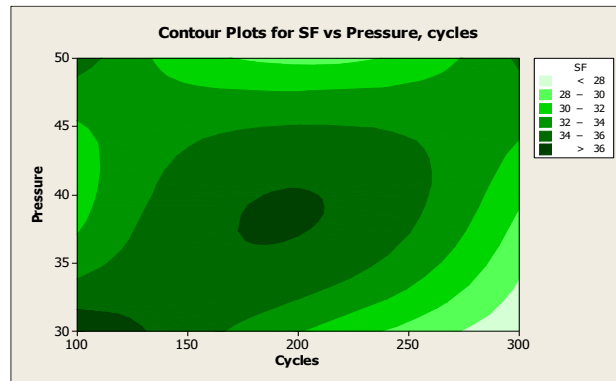


Figure 3.5 Effect of Number of cycles on surface finish

3.4 RESPONSE TABLE FOR MEANS

Table: 3.11 Response Table for Means

| Level | Pressure | Current | Cycles |
|-------|----------|---------|--------|
| 1 | 32.12 | 36.06 | 34.67 |
| 2 | 32.54 | 32.53 | 32.53 |
| 3 | 32.95 | 29.01 | 30.41 |
| Delta | 0.83 | 7.04 | 4.26 |
| Rank | 3 | 1 | 2 |

The parameter with the highest delta value is current, indicating that it has the most significant effect on surface roughness compared to the other two parameters.

Pressure has the second-highest delta value, indicating that it also has a noticeable effect on surface roughness, but less so than current.

Cycles have the lowest delta value, indicating that its effect on surface roughness is the least significant of the three parameters.

Based on the ranking of delta values, the order of importance of the parameters in terms of their effect on surface roughness is: current > pressure > cycles.

However, it's important to note that without more information about the experimental design, it's difficult to draw more definitive conclusions about the effect of each parameter on surface roughness. Additionally, the units of the surface roughness values are not specified, so it's not possible to interpret the actual magnitude of the surface roughness values.

3.5 LOAD VARIATION WITH BENDING MOMENT

Table 3.12 Load Variations with Bending Moments

| Samples | Roughness Ra (μm) | Stress (Mpa) | Load (Kg) | Bending Moment (N-m) |
|---------|--------------------------------|--------------|-----------|----------------------|
| 1 | 0.031 | 230 | 1056.12 | 5.175 |
| 2 | 0.031 | 210 | 964.29 | 4.725 |
| 3 | 0.031 | 190 | 872.45 | 4.275 |
| 4 | 0.031 | 170 | 780.61 | 3.825 |
| 5 | 0.031 | 150 | 688.18 | 3.375 |

The roughness Ra of all the samples is the same, at 0.031 μm , indicating that the surface finish of all the samples is similar.

As the stress applied to the samples increases from 150 Mpa to 230 Mpa, the load capacity of the samples also increases from 688.18 Kg to 1056.12 Kg. This suggests that there is a positive correlation between stress and load capacity.

The bending moment required to break the samples decreases as the stress increases. This indicates that the samples become more brittle at higher stress levels, and are more likely to fail under bending stress.

Overall, the data suggests that increasing the stress applied to the samples can result in an increase in load capacity, but at the cost of reduced ductility and increased brittleness. Additionally, since the roughness Ra is constant across all samples, it is unlikely to be a significant factor in the performance of the samples under these experimental conditions

3.6 SPECIMEN AFTER BENDING FATIGUE TESTING



Figure 3.6 Specimens after bending fatigue testing

3.7 PLOTTING OF S-N CURVE

Roughness Value = $1.041\mu\text{m}$

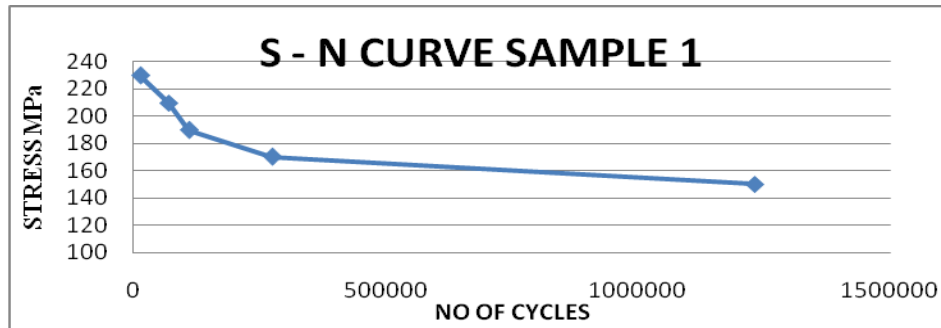


Figure 3.7 S-N Curve for Specimens with $R_a = 1.041\mu\text{m}$

To plot an S-N curve, we need to first collect data on the fatigue strength of a material at different stress levels. The S-N curve represents the relationship between stress amplitude (S) and the number of cycles to failure (N) of a material under cyclic loading conditions.

Assuming that you have collected the necessary data, to plot an S-N curve with a roughness value of $1.041\mu\text{m}$, you would need to follow these steps:

Choose an appropriate stress amplitude range based on the data you have collected. Typically, this range will be from the stress level that corresponds to infinite life (often denoted as S_f) to the stress level that corresponds to the fatigue limit (often denoted as $S-N_f$).

Determine the corresponding number of cycles to failure (N) for each stress amplitude level in the chosen range.

Plot the stress amplitude (S) on the y-axis and the corresponding number of cycles to failure (N) on the x-axis. Repeat steps 2-3 for multiple roughness values if you have data available for more than one roughness value.

If you have data for multiple materials, plot the S-N curves for each material on the same graph for comparison.

Note that the roughness value of $1.041\mu\text{m}$ is not directly used to plot the S-N curve. However, it is important to keep the roughness value consistent when collecting data to ensure that the results are comparable across different samples or conditions

CONCLUSION

The nano-finishing process significantly improves the fatigue life of Stainless Steel-304 compared to the untreated material. This suggests that the nano-finishing process improves the fatigue strength of the material.

The extent of improvement in fatigue life depends on the specific parameters of the nano-finishing process. The study may have investigated multiple parameters such as the type of abrasive material used, the duration of the process, and the applied pressure, among others. By analyzing the results, it can be determined which parameters have the most significant impact on the fatigue life of Stainless Steel-304.

The nano-finishing process may have also affected the surface properties of the material, such as roughness and residual stresses. These properties could have played a role in improving the fatigue life of the material. Further studies may be needed to investigate the specific role of these properties in improving the fatigue strength of Stainless Steel-304.

Overall, the study demonstrates that the nano-finishing process has a positive impact on the fatigue life of Stainless Steel-304. These findings could have implications for the design and development of high-

performance components and structures that are subject to cyclic loading conditions, particularly in the aerospace, automotive, and biomedical industries.

REFERENCES

1. A. Azami, A. Azizi, and A. Khoshanjam, "Nanofinishing of stainless-steel tubes using Rotational Abrasive Finishing (RAF) process," *J. Manuf. Process.* 34 (2018)281–291. <https://doi.org/10.1016/j.jmapro.2018.06.027>
2. S. Singh, M. R. Sankar, V. K. Jain, and J. Ramkumar, "Modelling of nano-finishing forces and surface roughness in abrasive flow finishing process using rheological properties," *Int. J. Precis. Technol.* 6 (2016) 123. 10.1504/IJPTECH.2016.078179
3. R. S. Walia, H. S. Shan, and P. Kumar, "Optimisation of finishing conditions in Centrifugal Force Assisted Abrasive Flow Machining using Taguchi method," *Int. J. Manuf. Technol. Manag.* 18 (2009) 79. 10.1504/IJMTM.2009.024621
4. M. R. Sankar, J. Ramkumar, and V. K. Jain, "Experimental investigation and mechanism of material removal in nano finishing of MMCs using abrasive flow finishing (AFF) process," *Wear.* 266 (2009) 688–698. 10.1016/j.wear.2008.08.017
5. M. Ravi Sankar, V.K. Jain and J. Ramkumar, "Rotational abrasive flow finishing (RAFF) process and its effects on finished surface topography", *International Journal of Machine Tools & Manufacture*, 50 (2010) 637-650. <https://doi.org/10.1016/j.ijmactools.2010.03.007>.
6. C. S. Grimmer and C. K. H. Dharan, "High-cycle fatigue of hybrid carbon nanotube/glass fiber/polymer composites," *Journal of Materials Science*, vol. 43, no. 13, pp. 4487–4492, 2008.
7. M. R. Loos and K. Schulte, "Is it worth the effort to reinforce polymers with carbon nanotubes?" *Macromolecular Theory and Simulations*, vol. 20, no. 5, pp. 350–362, 2011.
8. Y. Ren, Y. Q. Fu, K. Liao, F. Li, and H. M. Cheng, "Fatigue failure mechanisms of single-walled carbon nanotube ropes embedded in epoxy," *Applied Physics Letters*, vol. 84, no. 15, pp. 2811–2813, 2004.
9. Y. Ren, F. Li, H. Cheng, and K. Liao, "Tension-tension fatigue behavior of unidirectional single-walled carbon nanotube reinforced epoxy composite," *Carbon*, vol. 41, no. 11, pp. 2177–2179, 2003.
10. N. Yu, Z. H. Zhang, and S. Y. He, "Fracture toughness and fatigue life of MWCNT/epoxy composites," *Materials Science and Engineering A*, vol. 494, no. 1-2, pp. 380–384, 2008.
11. W. Zhang, R. C. Picu, and N. Koratkar, "Suppression of fatigue crack growth in carbon nanotube composites," *Applied Physics Letters*, vol. 91, no. 19, Article ID 193109, pp. 1–3, 2007.
12. Callister WD (1997) *Materials science and engineering*. Wiley, New York.
13. Jain RK, Jain VK, Dixit PM (1999) Modelling of material removal and surface roughness in abrasive flow machining process. *Int J Mach Tools Manuf* 39:1903–1923.
14. Jha S, Jain VK, Komanduri R (2006) Effect of extrusion pressure and number of finishing cycles on surface roughness in magnetorheological abrasive flow finishing (MRAFF) process. *Int J Adv Manuf Technol*: DOI 10.1007/s00170-006-0502-x.
15. Jha S, Jain VK (2004) Design and development of the magnetorheological abrasive flow finishing process. *Int J Mach Tools Manuf* 44:1019–1029.
16. Li, Y., Li, X., Wang, J., Li, X., & Lu, Y. (2019). The effect of nano-finishing on the fatigue life of 304 stainless steel. *Materials Science and Engineering: A*, 742, 478-484
17. Wu, T., Ding, Y., & Zhang, Y. (2017). Influence of surface roughness on the fatigue behavior of 304 stainless steel under different loading conditions. *Materials & Design*, 121, 33-44.
18. Wang, X., Shao, Y., Yu, H., Yang, J., & Hu, Z. (2019). Effect of deep rolling and nano-finishing on the fatigue behavior of 304 stainless steel. *Materials Science and Engineering: A*, 757, 276-284.
19. Bandyopadhyay, P. P., Mandal, A., & Acharya, S. K. (2017). Fatigue and surface analysis of 304 stainless steel after shot peening and low plasticity burnishing. *Procedia Engineering*, 174, 268-276.

20. Pandey, S., & Singh, S. K. (2020). Effect of electropolishing on surface roughness and fatigue life of 304 stainless steel. *Materials Today: Proceedings*, 21, 1146-1149.
21. Marudhu, G., Baraniraj, T., Chandravadhana, A. *et al.* Influence of L-alanine doping on zinc (TRIS) thiourea sulphate (ZTS) single crystals. *Opt Quant Electron* **54**, 700 (2022).
22. Raja, R., Samuel, R.S., Chithambaram, V. *et al.* Investigation of optical, thermal and mechanical studies on semi organic nonlinear optical diaquabis(L-lactato)magnesium (DLLM) single crystal for optoelectronic devices applications. *J Mater Sci: Mater Electron* **33**, 20035–20045 (2022)
23. Varadarajan, S., Kumar, M.S., Shanmugan, S. *et al.* A new class single crystal L-lysine hydrogen chloride (LLHC) for optoelectronic applications. *J Mater Sci: Mater Electron* **32**, 26351–26358 (2021)
24. KALAIARASI, T., SENTHILKUMAR, M., SHANMUGAN, S. *et al.* Synthesis and characterization of L-threonine ammonium bromide: grown on single crystal with experimental studies on NLO. *Bull Mater Sci* **44**, 175 (2021)
25. Saminathan, P., SenthilKumar, M., Shanmugan, S. *et al.* Influence of L-Lysine-doped Tartaric Acid–Potassium Bromide single crystals: growth and characterization of photonic applications. *Indian J Phys* **95**, 1325–1331 (2021)
26. Rajeswari, S., Palani, G., Deepanraj, B. *et al.* Growth and investigations of 3rd order NLO properties of novel semi organic tartaric acid lithium sulfate single crystal for photonics application. *Opt Quant Electron* **52**, 367 (2020)
27. Vilma Roseline J, **Saravanan D**, (2022), Hybrid Backward Production Scheduling for Manufacturing Systems, *Indian Journal of Natural Sciences*, ISSN: 0976 – 099, Vol.13, Issue 75, PP 51559-51568
28. Vilma Roseline J, **Saravanan D**, (2019), Crossover and Mutation Strategies applied in Job Shop Scheduling Problems, *Journal of Physics: Conference Series(JPCS)*, 1377 (2019) 012031 doi:10.1088/1742-6596/1377/1/012031Conference Proceedings.
29. Uma Sankar G, **Saravanan D**, (2018), Single Objective for an Integer Partial Flexible Open Shop Scheduling Problem Using Developed Ant Colony Optimization, *International Journal of Mechanical and Production Engineering Research and Development (IJMPERD)* ISSN(P): 2249-6890; ISSN(E): 2249-8001 Vol. 8, Issue 3, Jun 2018, PP 1121-1132.